

# Maximizing hydrogen production through photovoltaic generator by using improved incremental conductance algorithm with proportional integral PI controller

Absane Sara<sup>1\*</sup> , Outzourhit Abdelkader<sup>2</sup> , Amatoul Fatima-Zahra<sup>3</sup> .

<sup>1,3</sup>Department of Physical and Science Laboratory of Materials, Energy and Environment, Cadi Ayyad University, Faculty of Science Semlalia, Marrakech, Morocco.

<sup>2</sup>Department of Physical and Science Laboratory of Environmental Science and Sustainable Development, Cadi Ayyad University, High School of Technology Essaouira, Morocco.

E-mail: <sup>1</sup>[saraabssane.essma@gmail.com](mailto:saraabssane.essma@gmail.com).

## ARTICLE INFO.

Article history:

Received 25 Jul 2024

Received in revised form 1 Aug 2024

Accepted 16 Nov 2024

Available online 17 Nov 2024

## KEYWORDS

Hydrogen production, DC-DC step-down converter; photovoltaic generator, Electrolyser, Incremental conductance, PI controller. MATLAB/Simulink.

## ABSTRACT

Effectively storing energy for prolonged periods poses a primary challenge for renewable and innovative energy sources. This research focuses on two key objectives: first, converting photovoltaic (PV) voltage to the necessary level for electrolysis through a buck converter, and second, utilizing a maximum power point tracking (MPPT) method to optimize the solar generator's efficiency. The simulation of the solar-driven buck converter for the electrolysis load was carried out using MATLAB/Simulink, integrating an Incremental Conductance (INC) MPPT algorithm with a PI controller for system optimization. The simulation results reveal the stabilization of both the generated power from the PV system and the load voltage. Significantly, the proposed system achieves an efficiency surpassing 90% under high irradiance levels.

\*Corresponding author.

DOI: <https://doi.org/10.51646/jsesd.v13i2.229>

This is an open access article under the CC BY-NC license ([http://Attribution-NonCommercial 4.0 \(CC BY-NC 4.0\)](http://Attribution-NonCommercial 4.0 (CC BY-NC 4.0))).



## تعظيم إنتاج الهيدروجين باستخدام مولد كهروضوئي من خلال تحسين خوارزمية التوصيل المتزايد مع التحكم التناسبي التكاملي (PI)

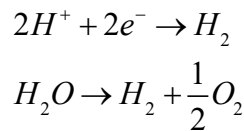
عبسان سارة، أوتزورهييت عبد القادر، أماتول فاطمة الزهراء.

**ملخص:** يواجه تخزين الطاقة بشكل فعال لفترات طويلة تحديات رئيسية لمصادر الطاقة المتجددة و المبتكرة يركز هذا البحث على هدفين رئيسيين: أولاً تحويل الجهد الكهربائي للخلايا الشمسية الى المستوى اللازم لعملية التحليل الكهربائي من خلال محول DC-DC وثانياً استخدام خوارزمية Incremental Conductance (INC) MPPT algorithm مع متحكم PI لتتبع لنقطة القدرة القصوى لتحسين كفاءة مولد الطاقة الشمسية تم تنفيذ محاكاة محول الجهد المدعوم بالطاقة الشمسية لتشغيل التحليل الكهربائي باستخدام برنامج MATLAB/Simulink. أظهرت نتائج المحاكاة استقرار الطاقة المولدة من نظام الخلايا الشمسية وجهد الحمل حيث حقق النظام المقترح كفاءة تفوق 90% تحت مستويات عالية من الاشعة الشمسية.

**الكلمات المفتاحية:** إنتاج الهيدروجين، محول خافض للتيار المستمر DC-DC، مولد كهروضوئي، محلل كهربائي، خوارزمية التوصيل المتزايد، متحكم تناسبي تكاملي MATLAB/Simulink، (PI).

### 1. INTRODUCTION

Conventional energy systems are increasingly being replaced due to the need for renewable energy, primarily because of their eco-friendly characteristics. Unlike fossil fuels [1], renewable sources like solar and wind generate electricity without emitting harmful greenhouse gases, thus helping to alleviate the negative impacts of climate change.[2], [3]. Moreover, renewable energy contributes to energy security by diversifying energy resources and reducing dependence on finite and sensitive resources. Additionally, the sustainable nature of renewable resources ensures a long term energy supply, leading to economic stability[4]. Combining solar energy with electrolysis is a crucial strategy in advancing sustainable and carbon neutral energy systems. Research studies emphasize the importance of integrating solar photovoltaic (PV) technology with electrolyzers to produce green hydrogen efficiently[5]. In this process, solar panels capture energy from the sun, converting solar radiation into electricity. This electricity is then used to power the electrolyzer, which employs electrical energy to split water (H<sub>2</sub>O) into hydrogen (H<sub>2</sub>) and oxygen (O<sub>2</sub>) gases, following the chemical reaction:



This integrated system allows the use of solar power in hydrogen production, providing a sustainable and clean energy solution. Solar electrolysis systems have been suggested to harness the intermittent nature of solar power[6], addressing the challenge of matching electricity generation with demand. Furthermore, As the shift towards renewable energy intensifies, the integration of solar power with electrolysis is recognized as a crucial strategy for efficiently storing and harnessing solar energy in a flexible environmentally and friendly way [7]. The DC-DC step down converter plays a crucial role in optimizing the energy transfer between an electrolyzer and a photovoltaic (PV) system, contributing to the overall efficiency and stability of the renewable energy setup. Positioned as an intermediate device, the DC-DC buck converter facilitates the conversion of higher voltage from the PV system to a lower, more suitable voltage for the electrolyzer. This conversion is essential for maintaining the electrolyzer's operational parameters, ensuring that it receives the required voltage and current for efficient electrolysis processes. By dynamically adjusting the voltage levels, the DC-DC buck converter aids in synchronizing the intermittent nature of solar energy production with the constant energy demand of the electrolysis process, thereby enhancing the overall performance and reliability of the integrated renewable energy

system. The converter's ability to regulate voltage levels contributes to minimizing energy losses and optimizing the utilization of the generated solar power, making it a vital component in the seamless integration of PV systems with electrolysis technologies for sustainable hydrogen production [8]. This integrated system enables the direct utilization of solar power for hydrogen production, offering a sustainable and clean energy solution. Several researchers have adapted the PV/Electrolyzer with DC-DC step down converter, such as Mustafa et al [9] who investigated a dc/dc buck converter connected with solar panels to power an electrolyzer to generate hydrogen. The converter could improve efficiency while maintaining a consistent output. Rahim et al[10]. improved the procedure of directly integrating solar panels to an electrolyzer. The efficiency of hydrogen production was enhanced by aligning the operating voltage of the PEM electrolyzer. The optimization method increased the electrolyzer's efficiency by up to 12%. Garrigos et al[11] . controlled the duty ratio of the DC-DC step down converter by adjusting the current delivered to the electrolyzer and optimizing the Maximum Power Point Tracking (MPPT) of the PV panels. Pathak et al[12] employed fuzzy logic control for MPPT in solar photovoltaic renewable energy systems, which they compared and examined with the Perturb and observe approach and incremental conductance. Pathak et al [13]. designed the P&O approach to reduce oscillations due to variations in insolation levels. This study focuses on enhancing the PV output power using improved Incremental Conductance integrated with a Proportional-Integral (PI) controller to maximize hydrogen generation via water electrolysis. This paper also discusses the hydrogen compression and storage process. A DC-DC step-down converter with MPPT control is employed to convert photovoltaic power for supplying the electrolysis process , Subsequently, the proposed PV/electrolyzer system is employed to analyze the impact of solar irradiation and temperature on the system's efficiency. The 8.5kW solar system demonstrates its capability to generate  $4.9 \times 10^{-6}$  kg/s of hydrogen under standard test conditions ( $G=1000\text{W/m}^2$ ,  $T=25^\circ\text{C}$ ). The organization of this paper is as follows: Section 2 presents the system description. The proposed MPPT based on an Incremental Conductance algorithm (INC) with a Proportional-Integral controller (PI) is discussed in Section 3. Section 4 covers the modeling of the electrolyzer with a compressor and hydrogen storage tank. Section 5 presents the results obtained using MATLAB/Simulink and the discussion part, In the final section, the conclusion is provided.

## 2. METHOD AND SYSTEM DESCRIPTION

The suggested system mainly comprises a photovoltaic system in which an MPPT technique is employed to maximize the solar output power integrated with a buck converter to adjust the duty cycle to reach the operating voltage of the Polymer electrolyte membrane electrolyzer and other auxiliaries components: compressor of hydrogen, tank storage as presented in figure1.

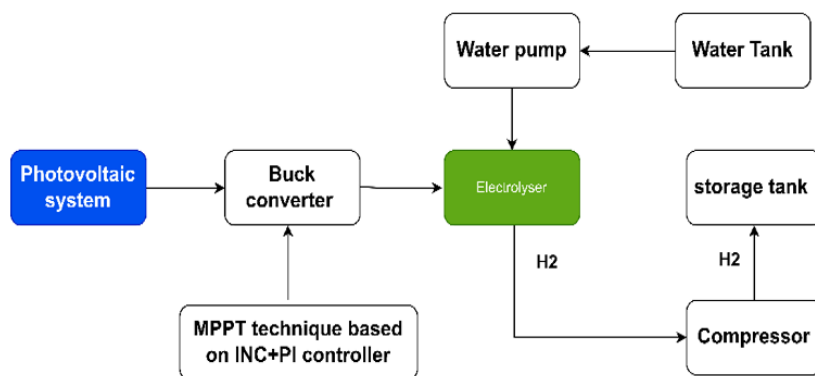


Figure 1. Model of described system PV/electrolyzer system with MPPT technique.

## 2.1. Modeling of solar panel

The cell circuit is modeled by a current source interconnected with a diode and two resistors in series and in parallel  $R_{series}$ ,  $R_{shunt}$  respectively. the mathematical model of the Photovoltaic generator is described by [14].

$$I_{pv} = I_{ph} - I_s \left[ e^{\frac{q(V_{pv} + R_{series} \cdot I_{pv})}{N_s \cdot K \cdot T \cdot \mu}} - 1 \right] \cdot \frac{V_{pv} + R_{series} \cdot I_{pv}}{R_{shunt}} \quad (1)$$

$$I_{ph} = \frac{G}{G_{STC}} \left( I_{s,STC} + K_T (T - T_{STC}) \right) \quad (2)$$

$$I_s = I_{RS} \left( \frac{T}{T_{STC}} \right)^3 \text{EXP} \left[ qE_G \cdot \frac{\left( \frac{1}{T_{STC}} - \frac{1}{T} \right)}{K \cdot T \cdot A} \right] \quad (3)$$

The global irradiation ( $W/m^2$ ) is divided into diffuse irradiation  $D$  and direct irradiation  $I$  as expressed by (4).

$$G = I + D \quad (4)$$

Where:

$I_{RS}$ : is the reverse saturation current (Amper).

$K_T$ : is the coefficient related to the temperature of the short circuit current of the PV cell.

$T$ : is the temperature (Kelvin).

$I_{S,STC}$ : current at standard test condition (Amper)

$G_{STC}$ : is the irradiation at standard test conditions.

$K$ : is the Boltzmann constant (Joule/kelvin).

$E_G$ : is the energy band gap (Joule).

$\mu$ : is the ideality factor.

$N_s$ : cells in series.

$A$ : is the surface area of the cell ( $m^2$ ).

$q$ : is the charge(C).

## 2.2. Maximum power point technique Incremental conductance (INC) and proportional Integrator PI.

### 2.2.1. Incremental conductance algorithm (INC)

The suggested improved Incremental Conductance (INC) algorithm is designed to determine the maximum power point (MPP) of a photovoltaic (PV) array under specific irradiation and temperature conditions.

At the MPP, the slope of the solar system power is equal to zero ( $dp/dv = 0$ ), positive to the left, and negative to the right [15]. This algorithm assesses the instantaneous conductance value ( $I/V$ ) along with the incremental conductance ( $\Delta I/\Delta V$ ) to evaluate the optimal operating point. the flowchart of the INC method is described in figure 2.

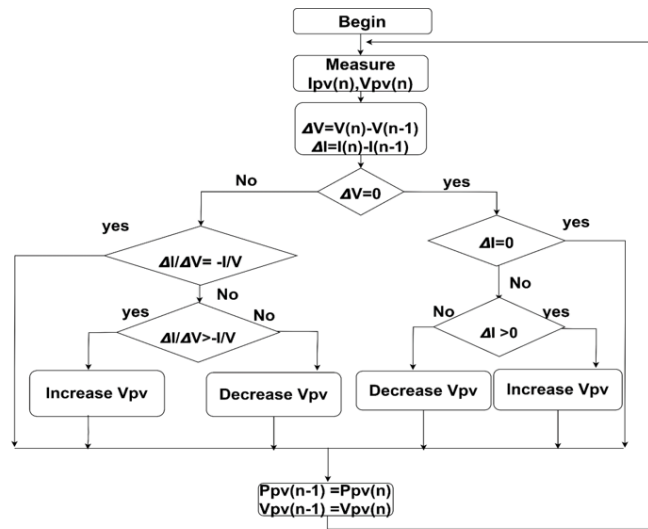


Figure 2. Flowchart of Incremental Conductance INC algorithm.

### 2.2.2. Proportional –integral controller PI

The Proportional-Integral (PI) control system operates as a feedback loop, determining the error signal by computing the difference between the system output and the desired value. Through the adjustment of parameters like the proportional coefficient  $k_p$ , and integral coefficient  $k_i$ , this control approach aims to achieve optimal outcomes.

The proportional element of the system responds to the instantaneous error between the desired and actual values, adapting the control output in direct proportion to this error, denoted as  $e(t)$ . While this ensures a rapid response to changes, it may lead to a persistent steady-state error. The integral controller  $k_i$ , effectively addresses steady-state errors, contributing to the elimination of such discrepancies in the system. The output of the controller PI value is determined as:

$$S(t) = K_p \cdot e(t) + k_i \int e(t) dt \quad (5)$$

As illustrated from figure 3, The error obtained from the  $(I/V) + (dI/dt)$ . Is minimised by the PI controller to generate a PWM signal to drive the converter.

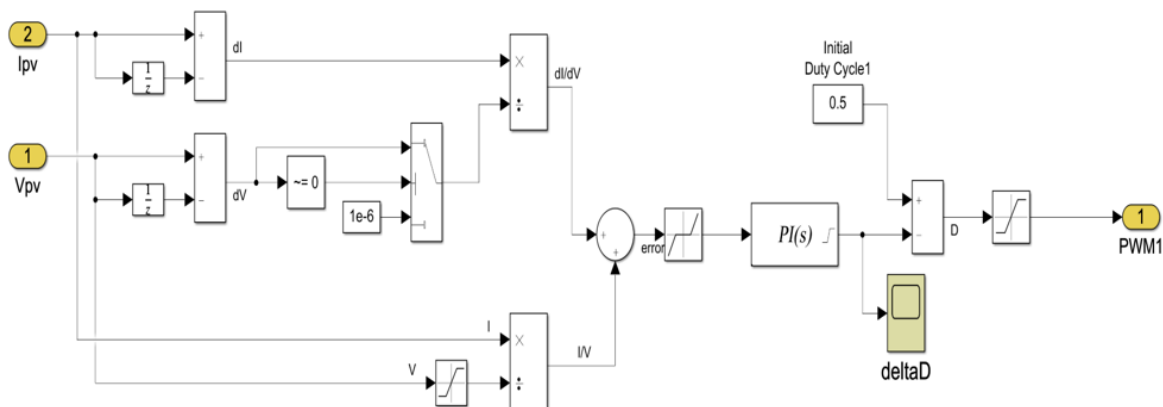


Figure 3. Block diagram of the INC with a PI controller.

### 2.3. DC-DC step down converter

The DC-DC step-down converter plays a crucial role in the proposed solar system by powering an electrolyzer. It accomplishes this task by converting the voltage generated by the PV panel to match the required electrolysis voltage level[17]. The MOSFET switch alternates between an active ON state and an inactive OFF state at a high frequency. When in the ON state, the switch is closed, allowing current to flow through the inductor. Subsequently, during the OFF state, the collapse of the magnetic field induces a voltage in the opposite direction across the inductor. This process facilitates the discharge of energy from the inductor, supplying continuous current to the load. The values of the converter's circuit input and output capacitor  $C_1$ ,  $C_2$  and inductor  $L$  were calculated by[18].

### 2.4. Electrolyzer

The water electrolysis process is a method of splitting water molecules into their elemental components, hydrogen and oxygen, through the application of an electric current. This electrochemical reaction takes place in an electrolytic cell containing water and electrodes. When an electric voltage is applied across the electrodes, water molecules undergo electrolysis, with the hydrogen ions ( $H^+$ ) migrating to the cathode and gaining electrons to form hydrogen gas ( $H_2$ ), while oxygen ions ( $O^{2-}$ ) move to the anode, releasing electrons and generating oxygen gas ( $O_2$ )[19].

Resulting in the following electrochemical reactions:

- **At the Cathode (Reduction):**

Hydrogen ions  $H^+$  migrate to the cathode, where they gain electrons to form hydrogen gas ( $H_2$ ):

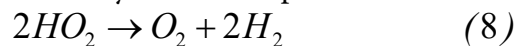


- **At the Anode (Oxidation):**



Oxygen ions  $O_2^-$  move to the anode, releasing electrons and generating oxygen gas ( $O_2$ ).

The overall reaction for water electrolysis can be represented as:



#### Voltage -Current (V-I) of the Electrolyzer

The performance of an electrolyzer is often represented by its V-I curve, which relates the applied voltage (V) to the current (I). This relationship accounts for the reversible voltage, ohmic losses, and activation losses. A general equation for the V-I curve is:

$$V = V_{rev} + \frac{r_1 + r_2 \cdot T}{B} \cdot I + s \cdot \log \left( \frac{\left( t_1 + \frac{t_2}{T} + \frac{t_3}{T^2} \right)}{B} \cdot I + 1 \right) \quad (9)$$

Where:

$V_{rev}$ : is the reversible cell voltage (Volts).

$r_1, r_2$ : are resistive coefficients dependent on temperature .

$I$ : the current (A).

$B, s, t_1, t_2, t_3$  are constants related to the cell design and electrochemical kinetics.

#### Hydrogen Production Rate

The hydrogen production rate  $\dot{n}_{H_2}$  (mole/s) in an electrolyzer is governed by Faraday's law, which states that flow rate of hydrogen produced is proportional to the current flowing through the cell.

The rate can be expressed as [22], [23]:

$$\dot{n}_{H_2} = \frac{\left(\frac{1}{B}\right)^2}{f_1 + \left(\frac{1}{B}\right)^2} \cdot f_2 \cdot \frac{I}{Z \cdot F} \quad (10)$$

Where:

I: is the current (A).

Z: the number of electrons during the process of water electrolysis ( 2 electrons for water electrolysis).

F: is Faraday's constant (96,485 C/mole).

### Water Consumption and Oxygen Production

The rates of water consumption and oxygen production are directly linked to the hydrogen production rate. For every mole of hydrogen produced, one mole of water  $n_{H_2O}$  is consumed, and half a mole of oxygen  $n_{O_2}$  is produced. This can be described by the stoichiometric relationship:

$$\dot{n}_{H_2} = 2\dot{n}_{O_2} = \dot{n}_{H_2O} \quad (11)$$

### Mass Flow Rate of Hydrogen

The mass flow rate in (kg/s) can be expressed as:

$$m_{H_2} = \frac{\left(\frac{1}{B}\right)^2}{f_1 + \left(\frac{1}{B}\right)^2} \cdot f_2 \cdot \frac{I}{Z \cdot F} \cdot c \cdot v_{std} \quad (12)$$

Where

$v_{std}$ : is the volume of an ideal gas at standard conditions (0.0224136 m<sup>3</sup>/mole).

$c$ : is the conversion constant ( 0.08988 kg/m<sup>3</sup>).

$f_1$  and  $f_2$  are coefficients that vary in function of temperature.

## 2.5. Compressor of hydrogen

Compressors play an important role to optimize storage space and increasing hydrogen energy density. The gas compressor's operating power can be expressed by [24] .

$$P_{el,comp} = \eta_{el} \cdot \eta_{comp} \cdot \dot{m}_{inlet} \frac{k}{k-1} \left[ \left( \frac{P_2}{P_1} \right)^{\frac{k-1}{k}} - 1 \right] \quad (13)$$

In which  $\eta_{el}$  is the electrical efficiency is chosen to be 50% and  $\eta_{comp}$  the compressor efficiency equal to 60%,  $T_1$  is the temperature of hydrogen at entrance (T= 25°C), and K denotes the heat capacity ratio for hydrogen (K= 1.4) , The inlet and outlet pressures of compressor denoted as  $P_1(Pa)$  and  $P_2(Pa)$  are chosen to be 10 bar to 150 bar respectively, along with  $\dot{m}_{inlet}$  (kg/s) is the hydrogen flow rate into the compressor.

### 2.6. Hydrogen Storage tank

The following formula describes the formula of hydrogen storage pressure[25].

$$P_b - P_{bi} = z \frac{m_{H_2} \cdot R \cdot T_b}{M_{H_2} \cdot V_B} = \frac{P_b \cdot V_m}{R \cdot T_b} \cdot m_{H_2} = V_{H_2} \cdot \rho_{H_2} \quad (14)$$

$P_b(Pa)$  presents the tank pressure,  $P_{bi} (Pa)$  indicates the initial tank pressure.  $R$  is the universal gas constant equal to 8.3144 (J/mol .K),  $T_b(K)$  indicates the operating temperature,  $V_B (m^3)$  is the tank volume,  $z$  is the compressibility factor, the characteristics of the tank are mentioned in table 1.

TABLE 1. Inputs parameters of haydroge storage tank [25].

Hydrogen tank characteristics	value
Maximum tank pressure	300 bar
Bottle volume	5m <sup>3</sup>
Initial SoC	50%
Operating temperature	20°C

### 3. RESULTS

The implemented configuration includes a PV system Soltech1STH-340-WH, by connecting five solar panels in series, and five panels connected in parallel, it forms an 8.5kW system. Each PV panel, produces 340 W individually, contributes to an output voltage of 210V and a current of 40.45A, a DC-DC buck converter designed as mentioned in table 2, to supply power to the electrolyzer which have the characteristics illustrated in table 3.

TABLE 2. Input parameters of step down converter and PI parameters.

Parameters	Value
$L$	2mH
$C_1$	1000μ F
$C_2$	14μF
Frequency	20KHZ
$K_p$	8
$K_i$	20

TABLE 3. Input parameters of step down converter.

Electrolyzer parameter	Value
$I$	0.01 A
$r_1$	3.538550 x 10 <sup>-4</sup>
$r_2$	-3.02150 x 10 <sup>-6</sup>
$s$	0.22396
$t_1$	5.13093
$t_2$	-2.40447 x 10 <sup>2</sup>
$t_3$	3.410251 x 10 <sup>3</sup>

This system maximizes operating power by integrating an enhanced MPPT method based on the incremental conductance algorithm with a Proportional-Integral (PI) controller. The simulation was performed using MATLAB/Simulink software as depicted in Figure 4.



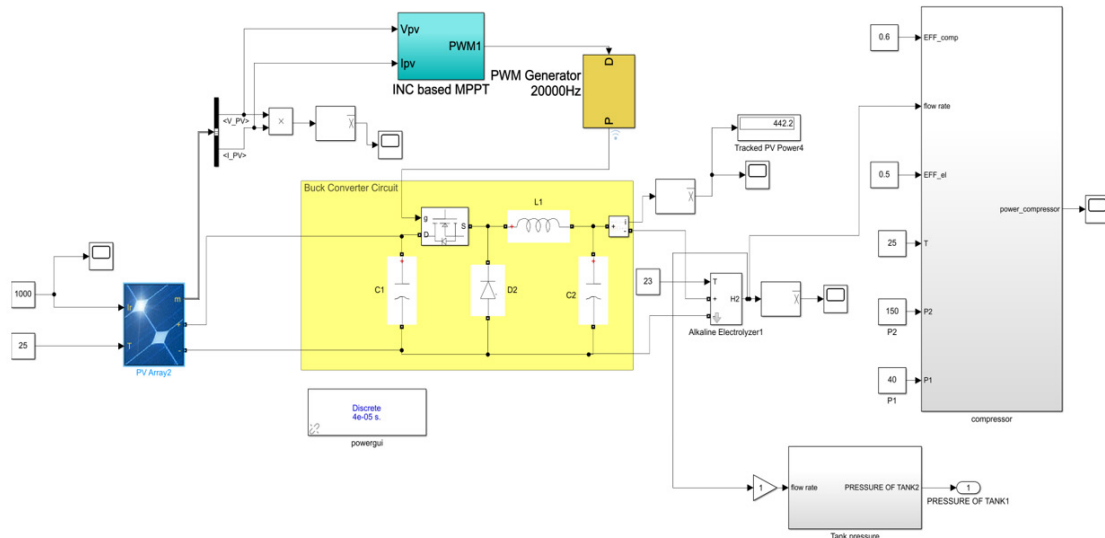


Figure 4. The overall system modelling in MATLAB/Simulink software.

From simulation results, when the temperature is  $T = 25^{\circ}\text{C}$  and irradiation  $G = 1000\text{W}/\text{m}^2$ , the voltage of the photovoltaic generator and the electrolyzer can quickly stabilize as the photovoltaic panels reached the maximum power point at the time  $t = 1\text{ms}$  which is equal to  $8450\text{W}$  as depicted in figure 5.

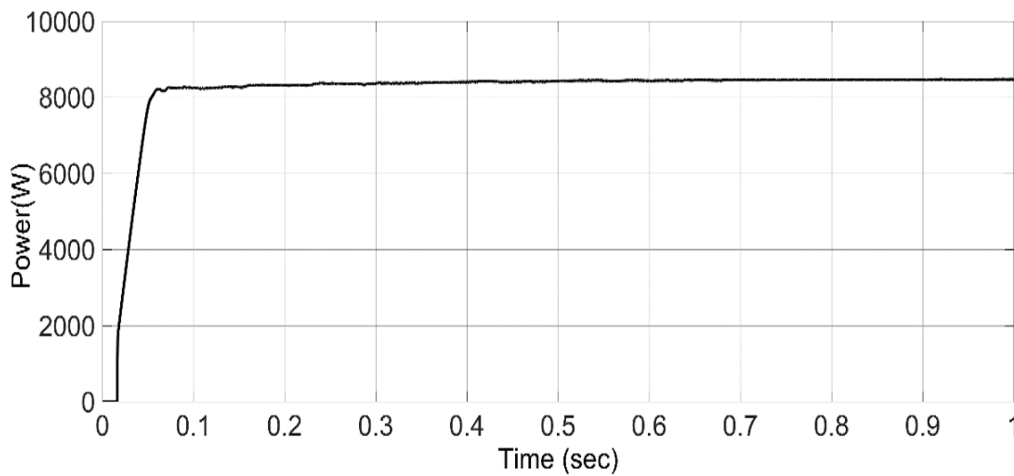


Figure 5. Solar generator Power at STC conditions.

while the electrolysis load voltage, current reached approximately  $16\text{V}$  and  $478\text{A}$  within  $0.15\text{s}$  receiving approximately an input power of  $7648\text{W}$  as shown in figure 6. These outcomes affirm that the system operates with an efficiency exceeding  $90\%$ . The degradation in power in the system are caused by losses in the step down converter.

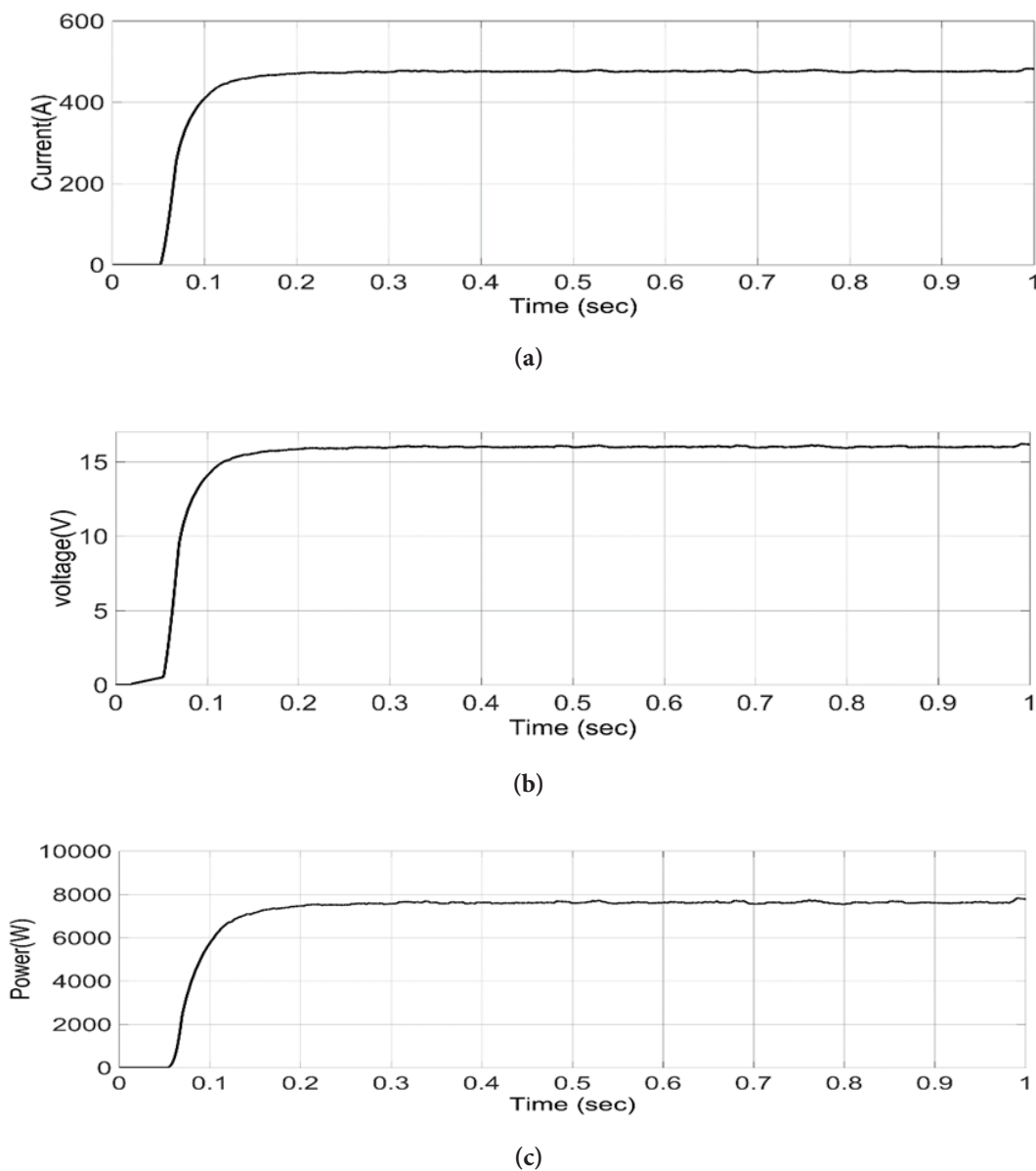


Figure 6. Electrolyzer (a). current, (b). voltage, (c). power.

### 3.1. Variable irradiation

In this case, variable irradiation levels are selected as illustrated in figure 7, we maintained temperature fixed at  $T=25^{\circ}\text{C}$ , when the irradiation decreases from  $1000\text{W}/\text{m}^2$  to  $200\text{W}/\text{m}^2$ , the power of the electrolyzer decreases as well the MPP is reached rapidly at a response time of (0.15s) without oscillation comparing to the conventional INC that required more response time (0.2s) and show some oscillations around MPP.

Moreover the power delivered to the electrolyser by the proposed INC with PI controller is the highest as seen in figure 8 , which explains the highest amount of the hydrogen produced compared to the conventional INC as mentioned in figure 9.

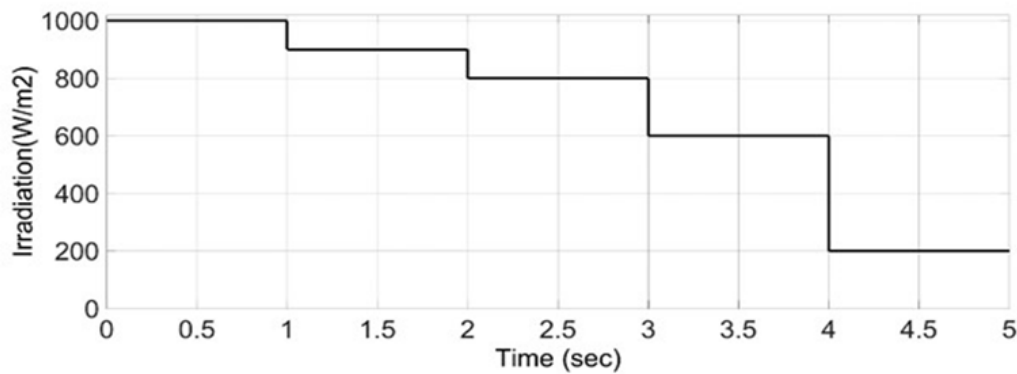


Figure 7. Variable irradiation.

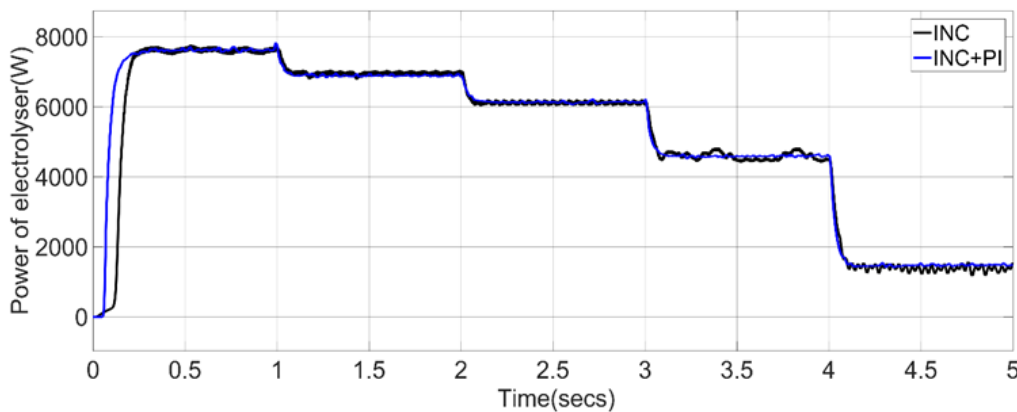


Figure 8. The power of the electrolyzer.

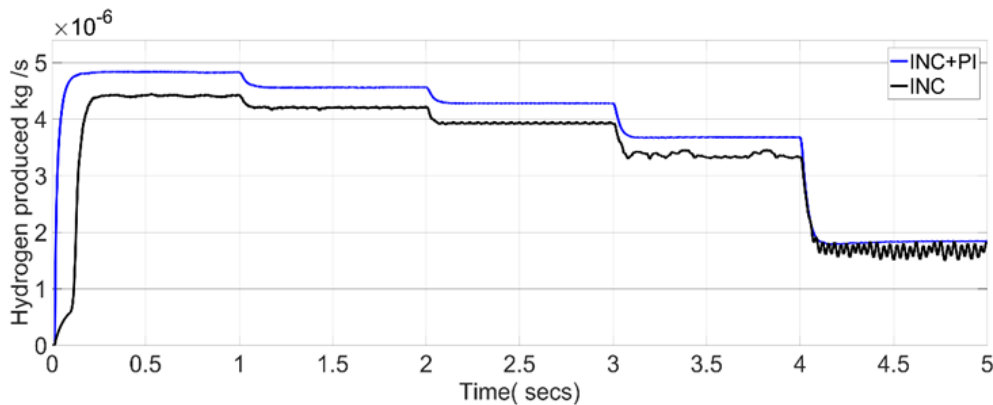


Figure 9. Hydrogen produced at variable irradiation.

The findings indicate that the efficiency exceeds 90% under conditions of high solar radiation levels, attributed to the converter operating at full capacity in such scenarios. nevertheless, higher temperatures conversely impact efficiency, but it is compensating by the increased solar irradiation.

### 3.2. Hydrogen production, compression and storage

The production of hydrogen reached about  $4.9 \times 10^{-6}$ kg/s at the high level of irradiation  $G=1000\text{W/m}^2$  and  $1.9 \times 10^{-6}$ kg/s at low irradiation ( $200\text{W/m}^2$ ) as seen in figure 9. After producing the hydrogen, it is compressed, thus the electrical power needed for the compressor is a function of the hydrogen produced given by (13).

The highest power of the compressor required is  $7.6 \times 10^4$ W as mentioned in Figure 10.

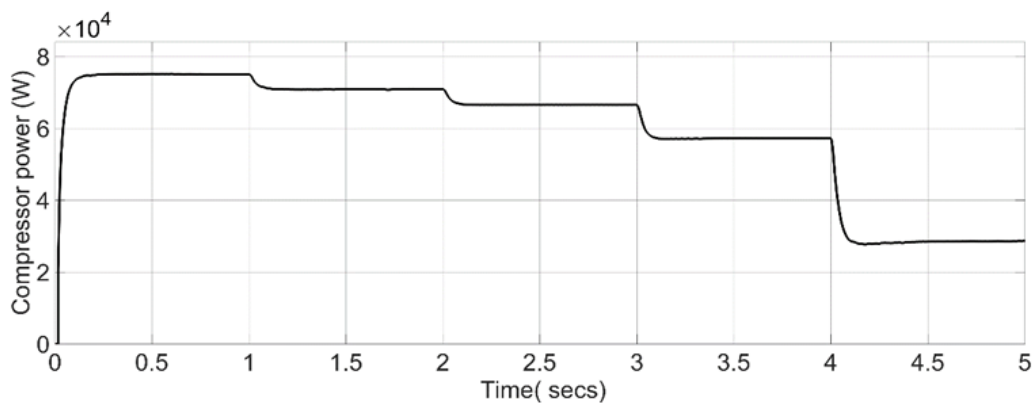


Figure 10. Power of the compressor.

After compressing the gas, it is stored in a pressurized bottle, the different parameters of the tank are described in Table 1 the pressure of the tank is proportional to the flow rate of hydrogen as it is given by (14) which explains the increase of the pressure as more and more hydrogen transferred to the tank as shown in figure 11 when the hydrogen production varies slowly at close irradiations levels the pressure slope remains approximately constant.

Table 4. The efficiency comparison table for various solar irradiation and temperature levels.

Temperature	25°C			45°C			10°C		
	Irradiation	Ppv (W)	Pload (W)	Efficiency (%)	Ppv (W)	Pload (W)	Efficiency (%)	Ppv (W)	Pload (W)
1000(W/m <sup>2</sup> )	8450	7641	90.42%	7819	6965	89.7%	8904	8130	91.3%
900(W/m <sup>2</sup> )	7626	6844	89.74 %	7064	6358	90%	8053	7274	90.03%
800(W/m <sup>2</sup> )	6789	6046	89.05%	6284	5636	89.6%	7166	6435	89.7%
600(W/m <sup>2</sup> )	5056	4487	88.7 %	4612	4081	88.4%	5454	4853	89.1%
200(W/m <sup>2</sup> )	1632	1416	86.7 %	1484	1259	84.8%	1528	1353	88.5%

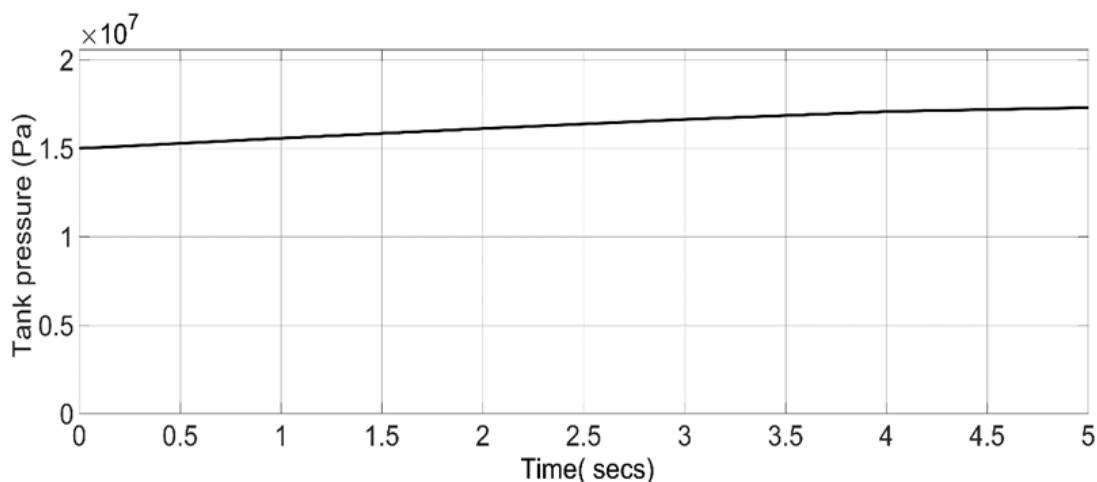


Figure 11. Pressure of the tank.

#### 4. CONCLUSION

this study provides significant insights into the integration of a photovoltaic (PV) system with a DC-DC buck converter and an electrolyzer, highlighting its potential for efficient green hydrogen production. By employing an enhanced (INC) MPPT method and a Proportional-Integral (PI) controller, the system successfully optimized PV output to meet the operational

requirements of the electrolyzer. The simulation results under standard conditions demonstrated the system's capacity to generate  $4.9 \times 10^{-6}$  kg/s of hydrogen, validating the feasibility of solar-driven hydrogen production as a sustainable energy solution. The importance of this research lies in its contribution to advancing renewable energy integration for hydrogen production, which is crucial for reducing reliance on fossil fuels and addressing global energy challenges. Despite the success, certain limitations must be considered. The system's performance was predominantly assessed under ideal conditions, limiting its ability to account for real-world environmental variability, such as rapid changes in solar irradiance and temperature. Therefore the Future work should address these limitations by enhancing the system's adaptability to diverse and unpredictable weather patterns. Incorporating advanced MPPT techniques, such as artificial neural networks (ANN), could improve the system's responsiveness to complex environmental changes. Additionally, integrating other renewable sources, such as wind energy, could provide a more stable and reliable energy supply. Finally, a detailed exploration of the hydrogen storage system's performance, including efficiency under varying load profiles, would deepen the understanding of the system's practical application and scalability.

**Authors contribution:** (SARA ABSSANE) developed the main idea for this research and was responsible for writing the majority of the manuscript. (Abdelkader Outzourhit) contributed by assisting with the interpretation of results and visualizing them. (Fatima Zahra Amatoul) helped prepare the figures and reviewed the manuscript.

**Funding:** This research was conducted without any external financial support.

**Data Availability Statement:** Not applicable.

**Conflicts of Interest:** The authors report no conflicts of interest.

**Acknowledgment:** We would like to convey our deep gratitude to the National Center for Scientific and Technical Research (CNRST) of Morocco for their crucial support and provision of resources during this research.

## REFERENCES

- [1] C. Yu, M. Moslehpour, T. K. Tran, L. M. Trung, J. P. Ou, and N. H. Tien, 'Impact of non-renewable energy and natural resources on economic recovery: Empirical evidence from selected developing economies', *Resources Policy*, vol. 80, p. 103221, Jan. 2023, doi: 10.1016/j.resourpol.2022.103221.
- [2] International Energy Agency, *Global EV Outlook 2019: Scaling-up the transition to electric mobility*. in *Global EV Outlook*. OECD, 2019. doi: 10.1787/35fb60bd-en.
- [3] K. Alanne and S. Cao, 'An overview of the concept and technology of ubiquitous energy', *Applied Energy*, vol. 238, pp. 284–302, Mar. 2019, doi: 10.1016/j.apenergy.2019.01.100.
- [4] Mahjabeen, S. Z. A. Shah, S. Chughtai, and B. Simonetti, 'Renewable energy, institutional stability, environment and economic growth nexus of D-8 countries', *Energy Strategy Reviews*, vol. 29, p. 100484, May 2020, doi: 10.1016/j.esr.2020.100484.
- [5] M. A. Abdelkareem et al., 'Optimized solar photovoltaic-powered green hydrogen: Current status, recent advancements, and barriers', *Solar Energy*, vol. 265, p. 112072, Nov. 2023, doi: 10.1016/j.solener.2023.112072.
- [6] C. Tarhan and M. A. Çil, 'A study on hydrogen, the clean energy of the future: Hydrogen storage methods', *Journal of Energy Storage*, vol. 40, p. 102676, Aug. 2021, doi: 10.1016/j.est.2021.102676.
- [7] T. Ikuerowo, S. O. Bade, A. Akinmoladun, and B. A. Oni, 'The integration of wind and solar power to water electrolyzer for green hydrogen production', *International Journal of Hydrogen Energy*, p. S0360319924005548, Feb. 2024, doi: 10.1016/j.ijhydene.2024.02.139.
- [8] S. Shiva Kumar and H. Lim, 'An overview of water electrolysis technologies for green hydrogen

- production', *Energy Reports*, vol. 8, pp. 13793–13813, Nov. 2022, doi: 10.1016/j.egy.2022.10.127.
- [9] M. E. Şahin, H. İ. Okumuş, and M. T. Aydemir, 'Implementation of an electrolysis system with DC/DC synchronous buck converter', *International Journal of Hydrogen Energy*, vol. 39, no. 13, pp. 6802–6812, Apr. 2014, doi: 10.1016/j.ijhydene.2014.02.084.
- [10] A. H. A. Rahim, A. S. Tijani, M. Fadhlullah, S. Hanapi, and K. I. Sainan, 'Optimization of Direct Coupling Solar PV Panel and Advanced Alkaline Electrolyzer System', *Energy Procedia*, vol. 79, pp. 204–211, Nov. 2015, doi: 10.1016/j.egypro.2015.11.464.
- [11] A. Garrigós, 'Combined maximum power point tracking and output current control for a photovoltaic-electrolyser DC/DC converter', *International Journal of Hydrogen Energy*.
- [12] P. K. Pathak and A. K. Yadav, 'Design of battery charging circuit through intelligent MPPT using SPV system', *Solar Energy*, vol. 178, pp. 79–89, Jan. 2019, doi: 10.1016/j.solener.2018.12.018.
- [13] P. K. Pathak, A. K. Yadav, and P. A. Alvi, 'Reduced oscillations based perturb and observe solar maximum power point tracking scheme to enhance efficacy and speed of a photovoltaic system'.
- [14] F. Saadaoui, K. Mammari, and A. Hazzab, 'Modeling of photovoltaic system with maximum power point tracking control by neural networks', *IJPEDS*, vol. 10, no. 3, p. 1575, Sep. 2019, doi: 10.11591/ijpeds.v10.i3.pp1575-1591.
- [15] K. K. Rout, D. P. Mishra, S. Mishra, and S. R. Salkuti, 'A painstaking analysis of various conventional and AI based MPPT approaches to the PV framework', *IJPEDS*, vol. 14, no. 4, p. 2338, Dec. 2023, doi: 10.11591/ijpeds.v14.i4.pp2338-2346.
- [16] V. Guida, D. Guilbert, and B. Douine, 'Literature Survey of Interleaved DC-DC Step-Down Converters for Proton Exchange Membrane Electrolyzer Applications', *TEEE*, vol. 3, no. 1, p. 33, Mar. 2019, doi: 10.22149/teee.v3i1.129.
- [17] D. Taufik, 'Practical Design of Buck Converter'.
- [18] M. Anam, H. I. Gomes, G. Rivers, R. L. Gomes, and R. Wildman, 'Evaluation of photoanode materials used in biophotovoltaic systems for renewable energy generation', *Sustainable Energy Fuels*, vol. 5, no. 17, pp. 4209–4232, 2021, doi: 10.1039/D1SE00396H.
- [19] F. Gambou, D. Guilbert, M. Zasadzinski, and H. Rafaralahy, 'A Comprehensive Survey of Alkaline Electrolyzer Modeling: Electrical Domain and Specific Electrolyte Conductivity', *Energies*, vol. 15, no. 9, p. 3452, May 2022, doi: 10.3390/en15093452.
- [20] M. C. Möller and S. Krauter, 'Hybrid Energy System Model in Matlab/Simulink Based on Solar Energy, Lithium-Ion Battery and Hydrogen', *Energies*, vol. 15, no. 6, p. 2201, Mar. 2022, doi: 10.3390/en15062201.
- [21] M. Rizwan, V. Alstad, and J. Jäschke, 'Design considerations for industrial water electrolyzer plants', *International Journal of Hydrogen Energy*, vol. 46, no. 75, pp. 37120–37136, Oct. 2021, doi: 10.1016/j.ijhydene.2021.09.018.
- [22] D. Martinez and R. Zamora, 'MATLAB Simscape Model of An Alkaline Electrolyser and Its Simulation with A Directly Coupled PV Module', vol. 8, no. 1, 2018.
- [23] J. Wei, Y. Gu, and X. Wu, 'A desulfurization fuel cell with alkali and sulfuric acid byproducts: a prototype and a model', *Sustainable Energy Fuels*, vol. 5, no. 14, pp. 3666–3675, 2021, doi: 10.1039/D1SE00659B.
- [24] J. Zou et al., 'Electrochemical Compression Technologies for High-Pressure Hydrogen: Current Status, Challenges and Perspective', *Electrochem. Energ. Rev.*, vol. 3, no. 4, pp. 690–729, Dec. 2020, doi: 10.1007/s41918-020-00077-0.
- [25] M.-R. Tahan, 'Recent advances in hydrogen compressors for use in large-scale renewable energy integration', *International Journal of Hydrogen Energy*, vol. 47, no. 83, pp. 35275–35292, Oct. 2022, doi: 10.1016/j.ijhydene.2022.08.128.